Alloying-driven phase stability in group-VB transition metals under compression

A. Landa,[1] P. Söderlind,[1] O. I. Velikokhatnyi,[2] I. I. Naumov,[3] A. V. Ruban,[4] O. E. Peil,[4,5] and L. Vitos[4,6]
[1]*Condensed Matter and Materials Division, Physical and Life Sciences Directorate, Lawrence Livermore National Laboratory, Livermore, California 94551, USA*
[2]*Department of Bioengineering, University of Pittsburgh, Pittsburgh, Pennsylvania 15261, USA*
[3]*Information and Quantum Systems Laboratory, Hewlett-Packard, Palo Alto, California 94304, USA*
[4]*Department of Materials Science and Engineering, Applied Materials Physics, Royal Institute of Technology, SE-100 44 Stockholm, Sweden*
[5]*Institute of Theoretical Physics, University of Hamburg, 20355 Hamburg, Germany*
[6]*Department of Physics and Materials Science, Division for Materials Theory, Uppsala University, SE-75121 Uppsala, Sweden*
(Received 14 July 2010; revised manuscript received 11 September 2010; published 20 October 2010)

The change in phase stability of group-VB (V, Nb, and Ta) transition metals due to pressure and alloying is explored by means of first-principles electronic-structure calculations. It is shown that under compression stabilization or destabilization of the ground-state body-centered-cubic (bcc) phase of the metal is mainly dictated by the band-structure energy that correlates well with the position of the Kohn anomaly in the transverse-acoustic-phonon mode. The predicted position of the Kohn anomaly in V, Nb, and Ta is found to be in a good agreement with data from the inelastic x-ray or neutron-scattering measurements. In the case of alloying the change in phase stability is defined by the interplay between the band-structure and Madelung energies. We show that band-structure effects determine phase stability when a particular group-VB metal is alloyed with its nearest neighbors within the same *d*-transition series: the neighbor with less and more *d* electrons destabilize and stabilize the bcc phase, respectively. When V is alloyed with neighbors of a higher (4*d*- or 5*d*-)transition series, both electrostatic Madelung and band-structure energies stabilize the body-centered-cubic phase. The opposite effect (destabilization) happens when Nb or Ta is alloyed with neighbors of the 3*d*-transition series.

DOI: 10.1103/PhysRevB.82.144114 PACS number(s): 61.50.Ks, 61.66.Dk, 62.50.−p, 71.20.Be

I. INTRODUCTION

Vanadium metal has been the subject of numerous experimental and theoretical studies due to its high superconducting transition temperature. Ishizuka *et al.*[1] found that for V the superconducting transition temperature, T_c=5.3 K, increases linearly with pressure reaching 17.2 K (the highest T_c among the elemental metals reported so far) at 1.2 Mbar. In addition, they also found a small steplike increase in T_c near 600 kbar.

In order to explore the response of electron-phonon interaction to high pressures, Suzuki and Otani[2] performed first-principles calculations of the lattice dynamics of V in the pressure range up to 1.5 Mbar. They found that the frequencies of the transverse-acoustic (TA) mode [ξ00] soften around $\xi=\frac{1}{4}$ with increasing pressure and become imaginary (unstable) at pressures higher than 1.3 Mbar, indicating a structural phase transition. Later this result was confirmed by other *ab initio* calculations.[3] On the experimental side, recently by using inelastic x-ray scattering technique Bosak *et al.*[4] discovered several anomalies in the phonon dispersion curve for V along high-symmetry directions. Among these anomalies was an upward bending of the TA mode along the Γ-H direction, [ξ00], around ξ=0.24—the anomaly that has been predicted theoretically in Refs. 2 and 3. The recent synchrotron x-ray diffraction measurements on V (Ref. 5) reported a new rhombohedral (*rh*) phase around 630–690 kbar that is in the same pressure range where a small steplike increase in T_c was observed.[1] Later theoretical studies confirm this finding and also suggest vanadium to return to the bcc phase around 2.5–3.2 Mbar.[3,6–8]

The phonon anomaly in the TA [ξ00] phonon branch of V was attributed to the existence of parallel pieces of the Fermi surface (FS) which causes a strong electronic response at the nesting wave vector that translates these pieces one to the other.[9] The same authors[9] also found that the nesting vector $\boldsymbol{q_n}$, spanning two flat pieces of the FS in the third band, already exists at zero pressure and leads to the Kohn anomaly in the TA [ξ00] phonon mode for small $q_n \approx 0.24(2\pi/a)$, where a is the lattice constant. Since in the long wavelength limit ($q \to 0$) the trigonal shear elastic constant, c_{44}, is related to the TA [ξ00] phonon frequency, $\omega(q)$, by a simple relation: $\rho\omega^2(q)/q^2 \to c_{44}$, the Kohn anomaly also softens this elastic constant making it negative in the pressure range 1.80–2.75 Mbar. The full potential linear muffin-tin orbitals[10] and projector augmented waves[11] calculations reveal the lower limit of this pressure interval as 1.2 Mbar and 0.8 Mbar, respectively. Verma and Modak[6] emphasized that the transition from the bcc to *rh* structure in V under compression could occur even before the trigonal shear elastic constant becomes negative. A similar conclusion was independently derived by Luo *et al.*[3]

The remaining group-VB transition metals, Nb and Ta, also represent the so-called hard superconductors[12] whose superconducting properties highly depend on their physical and chemical states. Niobium has the highest superconducting transition temperature, T_c=9.25 K, among the elemental metals at ambient pressure.[13] According to Matthias *et al.*,[14] Ta becomes a superconductor at $T_c \sim 3.39-4.48$ K. By using inelastic neutron scattering, Nakagawa and Woods[15] found a decrease (below the elastic constant line) in TA [ξ00] phonon frequencies for Nb around ξ=0.20 (compare with ξ=0.24 for

V). Woods[16] performed the frequency-wave-vector dispersion relation measurements in Ta using the inelastic neutron-scattering technique similar that was used in measurements for Nb.[15] His results showed strong analogies with previously measured Nb,[15] however, a drastic decrease below the elastic constant line for TA $[\xi 00]$ phonon mode, observed for Nb, was not detected.

The question whether the TA $[\xi 00]$ phonon anomaly in VB transition metals is indeed electronic in nature and connected with "nesting areas" of the Fermi surface can be answered by comparing the nesting vectors, $\boldsymbol{q_n}=2\boldsymbol{k}_F$, in all the VB metals with the positions of their phonon anomalies, either calculated or measured experimentally. Luckily, reliable experimental data exist on phonon dispersions in all three metals—V,[4] Nb,[15] and Ta,[16] and it is time to fill this gap.

Another task of this paper is to expand the study recently performed by Landa *et al.*[17] on stability in bcc transition metals due to alloying. In that letter the phase stability of group-VB (V, Nb, and Ta) transition metals was explored by first-principles electronic-structure calculations. The authors found that alloying with a small amount of a neighboring metal can either stabilize or destabilizes the body-centered-cubic relative to a lower symmetry rhombohedral phase. Further, when $3d$-V is alloyed with neighbors of higher d-transition series, the electrostatic Madelung energy dominates and stabilizes the bcc phase. In the present paper we expand the study[17] to the case of $4d$-Nb and $5d$-Ta and show how the phase stability of Nb changes when it is alloyed with neighbors of lower $3d$ (Ti, V, or Cr) or higher $5d$ (Hf, Ta, or W) metals as well as what happens with Ta when it is alloyed with neighbors of lower $3d$ and $4d$ transition metals.

Our paper is organized as follows. Pertinent details of methodology are given in Sec. II followed by results of the generalized susceptibility calculations for transition metals (V, Nb, and Ta) in Sec. III. Results on stability of the bcc alloys based on the VB transition metals are presented in Sec. IV. We present our general discussion in Sec. V followed by conclusions in Sec. VI.

II. METHODOLOGY

The calculations that we have referred to as exact muffin-tin orbitals (EMTOs) are performed using a scalar-relativistic Green's-function technique based on an improved screened Korringa-Kohn-Rostoker method.[18] For the exchange/correlation approximation, we use the generalized gradient approximation.[19] In order to treat compositional disorder the EMTO method is combined with the coherent potential approximation (CPA).[20] The calculations are performed for a basis set including valence $spdf$ orbitals, whereas the core states are recalculated at each iteration. Integration over the irreducible wedge of the Brillouin zone (IBZ) is performed using the special k points method[21] with 819 k points for the bcc lattice. The Green's function has been calculated for 60–80 complex energy points distributed exponentially on a semicircle with 3.0–4.1 Ry diameter enclosing the occupied states. These calculations include the on-site screened Coulomb potential and energy, which take care of the electrostatics in the single-site CPA.[22] The corresponding screening

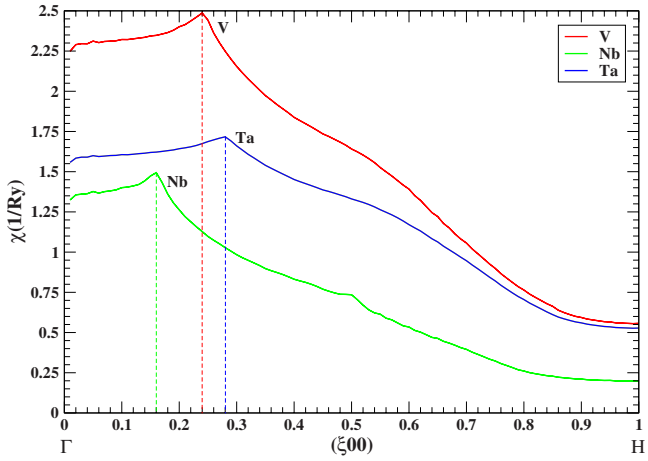

FIG. 1. (Color online) Partial (third→third intraband transition) electron susceptibility of V, Nb, and Ta calculated along the Γ-H direction at ambient pressure.

constants have been obtained in the locally self-consistent Green's-function[23] calculations for a 1024 atoms supercell that models the random equiatomic alloys. The equilibrium density and equation of state are obtained from a Murnaghan fit[24] to the total energy versus the lattice constant curve. It is should be stressed out that in the case of alloys we do not take into account the contributions to the total energy associated with the concentration expansion of the volume (homogeneous elastic energy) and static displacements of the atoms relative to the sites of an average "ideal" lattice (inhomogeneous elastic energy). The reasons are that we consider only weak solid solutions and, what it is more important, these contributions are only slightly structurally dependent and should not affect the analysis of structural stability. For the determination of the trigonal shear elastic constant, c_{44}, we apply a volume-conserving monoclinic distortion[25] and calculate the internal energy response. This setup requires 17 457 k points to perform integration over IBZ. The ground state for the rh phase is obtained by applying a volume conserving rhombohedral distortion[7] with 12 100 k points to perform integration over IBZ.

The generalized susceptibility of noninteracting electrons $[\chi(q)]$ is selected in order to detect the FS nesting. This function is calculated by using the highly precise analytic tetrahedron method.[26] In order to reach high precision in the $\chi(q)$ calculations, the IBZ lattice is divided into 16 000 tetrahedra.

III. GENERALIZED SUSCEPTIBILITY CALCULATION

The generalized susceptibility of noninteracting electrons $\chi(q)$ is closely related to the flat patches of the FS separated by some (nesting) vector $2\boldsymbol{k}_F$ peaking precisely at $\boldsymbol{q}=2\boldsymbol{k}_F$. Therefore, if the positions of some phonon anomalies of a metal system are closely correlated with the positions of maximum in $\chi(q)$, this would strongly indicate that these anomalies are of the Kohn nature.

Figure 1 shows the partial (due to the third→third electron intraband transition, see Refs. 9 and 10 for details) con-

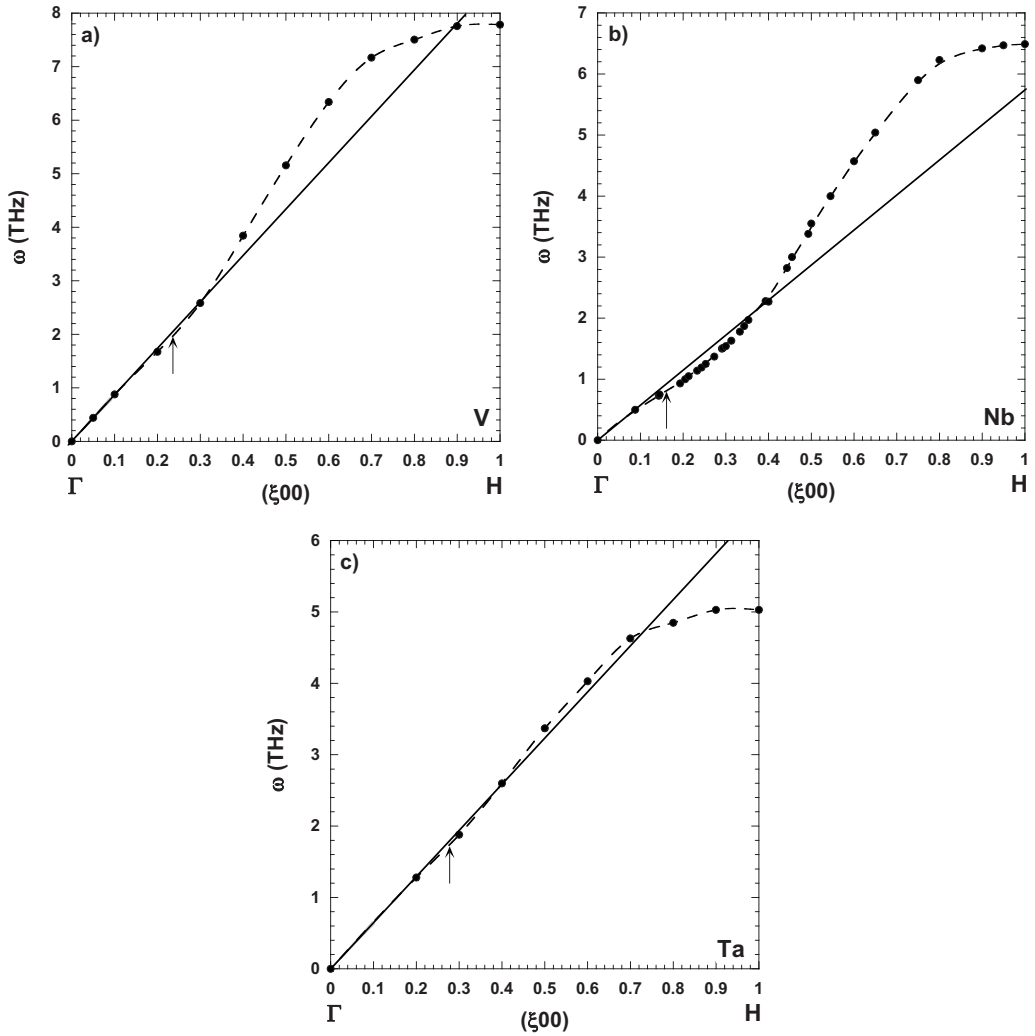

FIG. 2. The experimental phonon dispersion TA curve in [ξ00] direction for (a) V (Ref. 27), (b) Nb (Ref. 28), and (c) Ta (Ref. 16). The arrow indicates the Kohn anomaly obtained from *ab initio* calculations. The straight line represents the elastic constant line.

tribution to the generalized susceptibility, $\chi(q)$, of V, Nb, and Ta calculated along Γ-H (ξ00) direction at ambient pressure. As can be seen from this plot, the generalized susceptibility has a peak (due to the intraband nesting[9,10]) at $\xi \approx 0.24$, 0.16, and 0.28 for V, Nb, and Ta, respectively, indicating the position where the Kohn anomaly on the TA [ξ00] phonon branch is likely to occur. One can also see that this peak is more pronounced for V and Nb than for Ta suggesting that the Kohn anomaly is weaker in Ta than in V and Nb. In order to verify these results, we plot in Figs. 2(a)–2(c) the experimental phonon dispersion TA curve in [ξ00] direction for V, Nb, and Ta, respectively, using numerical data on the phonon frequencies from Refs. 16, 27, and 28. The location of the peak on the partial generalized susceptibility curve at ambient pressure, presented in Fig. 1, is marked by an arrow in Fig. 2. One can see that the position of the calculated peak in $\chi(q)$ is in fair accord with the point of the maximum deviation below the elastic constant line of the experimental TA [ξ00] phonon branch (the so-called phonon softening). In comparison with V, this deviation is observed to a larger and smaller extent for Nb and Ta, respectively.

Tracing the pressure dependence of the position of the maximum on the generalized partial susceptibility, we can plot (Fig. 3) the magnitude of the nesting vector, or the position of the Kohn anomaly, as a function of pressure. Our calculations show that the nesting vector decreases as pressure increases and the termination of a so-called "jungle-gym" hole tube occurs at between 2.25 and 2.50 Mbar, 0.60 and 0.75 Mbar, and 2.50 and 2.75 Mbar for V, Nb, and Ta, respectively. This is in a good agreement with results of Koči *et al.*[11] for V and Nb, although their calculations reveal a lower termination pressure for Ta (~2.25 Mbar).

IV. STABILITY OF THE BCC ALLOYS BASED ON V, Nb, AND Ta

Within the EMTO formalism, the total-energy, E_{tot}, can be expressed as the sum of two contributions: $E_{tot}=E_1+E_M$, where E_1 consists of all "local" (band-structure) contributions, $E_1=E_s+E_{intra}+E_{xc}$, such as the kinetic energy of non-interacting electron gas, E_s, the intracell electrostatic energy, E_{intra}, which is due to the electron-electron and electron-ion Coulomb interactions and also includes the screened Coulomb interactions in the case of the density-functional theory-CPA calculations, and the exchange and correlation

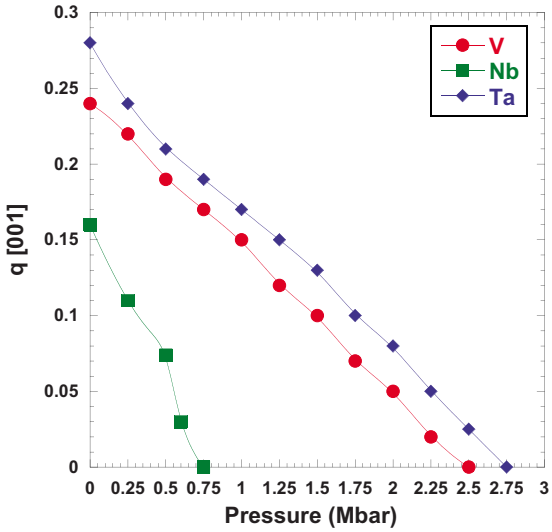

FIG. 3. (Color online) The magnitude of the nesting vector for V, Nb, and Ta as a function of pressure.

energy, E_{xc}. The remaining contribution, E_M, is the intercell Madelung energy. Note that the change in E_M due to alloying is proportional to the magnitude of the charge transfer between the atoms.

Table I lists the total-energy response ΔE_{tot} and its contributions, ΔE_1 and ΔE_M to a 1% monoclinic deformation, used for the trigonal shear elastic constant c_{44} calculations,[25] calculated for V, Nb, and Ta and their alloys with the IVB (Ti, Zr, and Hf), VB (V, Nb, and Ta), and VIB (Cr, Mo, and W) metals. Calculations are performed at the same atomic volumes indicated in Ref. 17. Negative values of the total-energy changes indicate mechanical instability of the bcc phase. The results for pure V, Nb, and Ta are presented in plain font. In the case of V(Nb, Ta)-based alloys the choice of the font depends on whether one observes stabilization or destabilization of the bcc phase: in the case of former (stabilization) scenario the results are presented in bold font and in the case of the later (destabilization) scenario the results are presented in italic font.

A. V-based alloys

The calculations for pure vanadium and V-based alloys are performed at the atomic volume $\Omega = 8.056$ Å^3 corresponding to the pressure of ~2.4 Mbar. According to Fig. 2 from Ref. 17, this pressure corresponds to the point of the maximum stability of the *rh* phase of vanadium in respect with the bcc phase—the ground-state phase at ambient pressure. Our previous calculations[17] predicted that vanadium undergoes a phase transition to the *rh* phase at ~0.6 Mbar reaching the maximum stability in the *rh* phase at ~2.4 Mbar before returning to the bcc phase at ~3.1 Mbar. The results for the $V_{95}Ti_{05}$, $V_{95}Cr_{05}$, and $V_{95}Nb_{05}$ alloys were already presented and discussed in Ref. 17: the band-filling argument (the number of valence electrons) is responsible, exclusively, for stabilization or destabilization of the bcc phase when V is alloyed with its neighbors within the same 3*d*-transition series, Cr or Ti, respectively, and stabilization of the bcc phase in the $V_{95}Nb_{05}$ alloy was explained due to the dominance of the electrostatic Madelung energy contribution to the total energy.

In addition to the $V_{95}Nb_{05}$ alloy, Table I also contains results in the total-energy response, ΔE_{tot}, and its contributions, ΔE_1 and ΔE_M, for alloys that vanadium forms with other 4*d* metals under consideration, Zr and Mo. Adding Zr or Mo to V significantly increases ΔE_{tot} thus implying stabilization of the bcc structure in the $V_{95}Zr_{05}$ or $V_{95}Mo_{05}$ alloys as was in the case of the $V_{95}Nb_{05}$ alloy. However for the $V_{95}Zr_{05}$ or $V_{95}Mo_{05}$ alloys, the increase in the band-energy contribution, ΔE_1, is, on average, 2.5 times larger than for the $V_{95}Nb_{05}$ alloy where this contribution is rather insignificant. Although the increase in ΔE_M, which, as was already mentioned, is proportional to the magnitude of the charge transfer on the vanadium atoms (see Table II), is significant: +0.0119 mRy, +0.0282 mRy, and +0.0301 mRy for the $V_{95}Mo_{05}$, $V_{95}Nb_{05}$, or $V_{95}Zr_{05}$ alloys, respectively, the increase in ΔE_1 for the $V_{95}Mo_{05}$ alloy (+0.0155 mRy) is even larger than that in ΔE_M (+0.0119 mRy). So we can no longer credit the electrostatic Madelung energy as the dominating factor in stabilization of the bcc structure in the

TABLE I. Contributions to the total-energy change (ΔE_{tot}) due to a 1% monoclinic deformation for V, Nb, and Ta, and their alloys. The results for pure V, Nb, and Ta are presented in plain font. In the case of V(Nb, Ta)-based alloys the choice of the font depends on whether one observes stabilization (bold) or destabilization (italic) of the bcc phase.

		IVB			VB			VIB		
						Metal				
Alloys		Ti 3*d*	Zr 4*d*	Hf 5*d*	V 3*d*	Nb 4*d*	Ta 5*d*	Cr 3*d*	Mo 4*d*	W 5*d*
3*d*-$V_{95}Me_{05}$	ΔE_1	*−0.2130*	**−0.1864**	**−0.1931**	−0.2010	**−0.1951**	**−0.1662**	**−0.1887**	**−0.1855**	**−0.1150**
	ΔE_m	**0.1895**	**0.2121**	**0.2044**	0.1820	**0.2102**	**0.2003**	**0.1823**	**0.1939**	**0.1915**
	ΔE_{tot}	*−0.0235*	**0.0257**	**0.0113**	−0.0190	**0.0151**	**0.0341**	**−0.0064**	**0.0084**	**0.0765**
4*d*-$Nb_{95}Me_{05}$	ΔE_1	*−0.0940*	*−0.1005*	*−0.0946*	*−0.0905*	−0.0860	**−0.0840**	*−0.0896*	**−0.0808**	**−0.0846**
	ΔE_m	*0.1839*	*0.1851*	*0.1861*	*0.1829*	0.1930	**0.1935**	*0.1786*	*0.1910*	*0.1850*
	ΔE_{tot}	*0.0899*	*0.0846*	*0.0915*	*0.0924*	0.1070	**0.1095**	*0.0890*	**0.1102**	*0.1004*
5*d*-$Ta_{90}Me_{10}$	ΔE_1	*−0.0188*	*−0.0223*	*−0.0169*	*−0.0181*	*−0.0103*	−0.0080	*−0.0161*	*−0.0130*	**0.0000**
	ΔE_m	*0.2194*	**0.2277**	**0.2289**	*0.2145*	**0.2316**	0.2250	*0.2117*	*0.2179*	0.2250
	ΔE_{tot}	*0.2006*	*0.2054*	*0.2120*	*0.1964*	**0.2213**	0.2170	*0.1956*	*0.2049*	**0.2250**

TABLE II. The calculated charge transfer induced on the V atoms in V-*M* alloys.

V-Ti (0.077)	V-V (0.000)	V-Cr (−0.070)
V-Zr (0.290)	V-Nb (0.247)	V-Mo (0.196)
V-Hf (0.306)	V-Ta (0.296)	V-W (0.277)

TABLE III. The calculated charge transfer induced on the Nb atoms in Nb-*M* alloys.

Nb-Ti (−0.146)	Nb-V (−0.247)	Nb-Cr (−0.336)
Nb-Zr (0.084)	Nb-Nb (0.000)	Nb-Mo (−0.081)
Nb-Hf (0.088)	Nb-Ta (0.046)	Nb-W (−0.005)

V 4*d*-transition-metal alloys as suggested in Ref. 17.

Adding 5*d* transition metals (Hf, Ta, and W) also stabilizes the bcc structure in the $V_{95}Hf_{05}$, $V_{95}Ta_{05}$, and $V_{95}W_{05}$ alloys. Although the increase in ΔE_M (+0.0095 mRy, +0.0183 mRy, and +0.0224 mRy for the $V_{95}W_{05}$, $V_{95}Ta_{05}$, or $V_{95}Hf_{05}$ alloys, respectively) plays an important role in stabilization of these alloys, a significant increase in ΔE_1 (+0.0086 mRy, +0.0348 mRy, and +0.0079 mRy for the $V_{95}W_{05}$, $V_{95}Ta_{05}$, or $V_{95}Hf_{05}$ alloys, respectively) takes place indicating that increases in ΔE_M and ΔE_1 are comparable for the $V_{95}W_{05}$ alloy. However, for the $V_{95}Ta_{05}$ alloy the increase in ΔE_1 is almost twice as large as that in ΔE_M. It appears that for only one alloy that V forms with 5*d* transition metals under consideration, $V_{95}Hf_{05}$, the electrostatic Madelung energy is the major factor in stabilization of the bcc structure.

B. Nb-based alloys

According to Fig. 1 from Ref. 17, the band-structure energy is also responsible for the pressure-induced shear softening in pure Nb at the pressure of ~0.5 Mbar that corresponds to the atomic volume $\Omega=14.92$ Å^3. This pressure was selected in previous calculations, Ref. 17, that explored the stability of bcc Nb upon alloying with its 4*d* neighbors Zr and Mo. It was discovered that there are obvious analogies when Nb is alloyed with its 4*d* neighbors (Zr and Mo) with the case of V alloyed with its 3*d* neighbors (Ti and Cr): the band-filling argument (the number of valence electrons) is responsible, exclusively, for stabilization or destabilization of the bcc phase when Nb is alloyed with its neighbors within the same 4*d*-transition series, Mo or Zr, respectively, and these results are presented in Table I.

In addition to the previous published[17] results on the $Nb_{95}Zr_{05}$, and $Nb_{95}Mo_{05}$ alloys, Table I contains the results of the present calculations of the energy change caused by 1% of the monoclinic deformation in the alloys that Nb forms with its 3*d* neighbors ($Nb_{95}Ti_{05}$, $Nb_{95}V_{05}$, and $Nb_{95}Cr_{05}$) and 5*d* neighbors ($Nb_{95}Hf_{05}$, $Nb_{95}Ta_{05}$, and $Nb_{95}W_{05}$). Calculations are performed at the same atomic volume $\Omega=14.92$ Å^3 corresponding to the pressure of ~0.5 Mbar that was used in the case of pure Nb, as wells as the $Nb_{95}Zr_{05}$ and $Nb_{95}Mo_{05}$ alloys.

In Table III we summarize the calculated charge transfers for Nb alloyed with the members of groups IVB, VB, and VIB. As one can see from this table, there is a significant negative charge transfer on the Nb atoms when Nb is alloyed with 3*d* metals (Ti, V, and Cr). The decrease in ΔE_M of pure Nb due to alloying is proportional to the absolute value of the charge transfer and appears to be −0.0091 mRy, −0.0101 mRy, and −0.0144 mRy for the $Nb_{95}Ti_{05}$, $Nb_{95}V_{05}$, and $Nb_{95}Cr_{05}$ alloys, respectively. There is also a decrease in ΔE_1 due to alloying: −0.0080 mRy, −0.0045 mRy, and −0.0036 mRy for the $Nb_{95}Ti_{05}$, $Nb_{95}V_{05}$, and $Nb_{95}Cr_{05}$ alloys, respectively, but in contrast to ΔE_M behavior, the drop in ΔE_1 decreases as the absolute value of the charge transfer on the Nb atoms increases Both the electrostatic Madelung and band-structure contributions determine the decrease in the total-energy, ΔE_{tot}, of Nb when it is alloyed with 3*d* transition metals but only for the $Nb_{95}Ti_{05}$ alloy these contributions are comparable in magnitude and the ΔE_M contribution plays the decisive role in destabilization of the $Nb_{95}V_{05}$ and $Nb_{95}Cr_{05}$ alloys.

Due to the similarity between 4*d* and 5*d* states, one can explain why an insignificant charge transfer occurs when 4*d*-Nb is alloyed with 5*d* metals Hf, Ta, and W (see Table III). Addition of 5 at. % Hf or W decreases the total-energy of pure Nb: $\Delta E_{tot}=-0.0155$ mRy and −0.0066 mRy for the $Nb_{95}Hf_{05}$ and $Nb_{95}W_{05}$ alloys, respectively, indicating a slight destabilization of the bcc phase. In the case of the $Nb_{95}Ta_{05}$ alloy the changes in both ΔE_M and ΔE_1 are positive: +0.0020 mRy and +0.0005 mRy, respectively, resulting in a slight ($\Delta E_{tot}=+0.0025$ mRy) stabilization of the bcc phase in the $Nb_{95}Ta_{05}$ alloy. In fact, only Mo and Ta stabilize the bcc structure in Nb but all the other metals under consideration behave differently where the largest degree of destabilization of the bcc phase in Nb takes place in the Nb-Zr system.

C. Ta-based alloys

In Ref. 17 we performed calculations of the energy change caused by 1% of the monoclinic deformation of pure bcc Ta, and its alloys with 5*d* neighbors ($Ta_{90}Hf_{10}$ and $Ta_{90}W_{10}$). The calculations were performed at the atomic volume $\Omega=14.68$ Å^3 corresponding to the pressure of ~0.65 Mbar, which is within the range of the c_{44} softening (Fig. 1, Ref. 17), and the results are presented in Table I. Again, there are analogies to the case of V and Nb when they are alloyed with their nearest neighbors within the same *d*-transition series: the band-filling argument (the number of valence electrons) is responsible, exclusively, for stabilization or destabilization of the bcc phase when Ta is alloyed with its neighbors within the same 5*d*-transition series, W or Hf, respectively,

In addition to the previous published[17] results on the $Ta_{90}Hf_{10}$, and $Ta_{90}W_{10}$ alloys, Table I contains the results of the present calculations of the energy change caused by 1% of the monoclinic deformation in the alloys that Ta forms with its 3*d* neighbors ($Ta_{90}Ti_{10}$, $Ta_{90}V_{10}$, and $Ta_{90}Cr_{10}$) and 4*d* neighbors ($Ta_{90}Zr_{10}$, $Ta_{90}Nb_{10}$, and $Ta_{90}Mo_{10}$). Calculations are also performed at the same atomic volume Ω

TABLE IV. The calculated charge transfer induced on the Ta atoms in Ta-*M* alloys.

Ta-Ti (−0.193)	Ta-V (−0.296)	Ta-Cr (−0.386)
Ta-Zr (0.041)	Ta-Nb (−0.046)	Ta-Mo (−0.127)
Ta-Hf (0.044)	Ta-Ta (0.000)	Ta-W (−0.051)

$=14.68$ Å^3 corresponding to the pressure of ~0.65 Mbar that was used in the case of pure Ta as well as the $Ta_{90}Hf_{10}$ and $Ta_{90}W_{10}$ alloys. In Table IV we summarize the calculated charge transfers for the Ta-based alloys. In analogy with Nb, there is a significant negative charge transfer on the host (Ta) atoms, when Ta is alloyed with 3*d* metals (Ti, V, and Cr) that provides a decrease in ΔE_M (−0.0056 mRy, −0.0105 mRy, and −0.0133 mRy for the $Ta_{90}Ti_{10}$, $Ta_{90}V_{10}$, and $Ta_{90}Cr_{10}$ alloys, respectively), which magnitude is proportional to the magnitude of the charge transfer (see Table IV). A decrease in ΔE_1 also takes place (−0.0108 mRy, −0.0101 mRy, and −0.0081 mRy for the $Ta_{90}Ti_{10}$, $Ta_{90}V_{10}$, and $Ta_{90}Cr_{10}$ alloys, respectively) but, again as it was in the case of Nb 3*d*-metals-based alloys, opposite to ΔE_M behavior: the drop in ΔE_1 decreases as the absolute value of the charge transfer on the Ta atoms increases. Consequently, there is a significant decrease (softening) in the total-energy change when Ta is alloyed with 3*d* metals (−0.0164 mRy, −0.0206 mRy, and −0.0214 mRy for the $Ta_{90}Ti_{10}$, $Ta_{90}V_{10}$, and $Ta_{90}Cr_{10}$ alloys, respectively). The largest decrease (~9.9%) occurs in the $Ta_{90}Cr_{10}$ alloy corresponding to the greatest negative charge transfer on the Ta atoms.

Finally, when Ta is alloyed with 4*d* metals (Zr and Mo) the largest drop in ΔE_M due to alloying (−0.0071 mRy) is observed in the $Ta_{90}Mo_{10}$ alloy where a relatively large negative charge transfer on the Ta atoms (−0.127) takes place. For the $Ta_{90}Zr_{10}$ alloy, where the charge transfer on the Ta atoms is positive (+0.041), the change in ΔE_M is positive (+0.0027 mRy). A decrease in ΔE_1 also occurs (−0.0143 mRy and −0.0050 mRy for the $Ta_{90}Zr_{10}$ and $Ta_{90}Mo_{10}$ alloys, respectively). This situation is similar to that when Ta is alloyed with 3*d* metals: the drop in ΔE_1 decreases as the absolute value of the charge transfer on the Ta atoms increases. The decrease in both ΔE_1 and ΔE_M in the $Ta_{90}Mo_{10}$ alloy and a significant decrease in ΔE_1, which overcomes a slight increase in ΔE_M in the $Ta_{90}Zr_{10}$ alloy, result in a decrease in the total-energy in the $Ta_{90}Mo_{10}$ and $Ta_{90}Zr_{10}$ alloys (−0.0121 mRy and −0.0116 mRy, respectively).

Alloying Ta with 10 at. % of Nb increases ΔE_M (+0.0066 mRy) and decreases ΔE_1 (−0.0023 mRy) resulting in increase in the total-energy, ΔE_{tot}, (+0.0043 mRy). The increase in ΔE_M occurs in spite of the small but negative charge transfer on the Ta atoms (−0.046). These values are numerically very small and represent an exception to the rule of thumb we have discovered: the sign (positive or negative) of the change in the ΔE_M due to alloying of two transition metals from the different *d* series corresponds to the sign (positive or negative) of the charge transfer on the host atoms. As a result, Nb joins W as the only metals under consideration that stabilize the bcc structure of Ta.

V. DISCUSSION

As was discovered in Ref. 17, small amounts (~3–5 at. %) of 4*d* and 5*d* metals are enough to stabilize the bcc structure of V. For these alloys the Madelung energy plays an important role in the stabilization, as opposed to the V-Ti and V-Cr alloys where it is negligible. This contrasting behavior is due to the inherent difference between 4*d* and 5*d* states compared to the 3*d* states. The former are more extended in space as are their corresponding charge distribution. Consequently, there is a larger charge transfer when V is alloyed with a 4*d* or 5*d* metal than with its neighbors Ti and Cr. As can be seen from Table II, the large and positive charge transfers means that more charge is supplied into the interstitial region thereby increasing the Madelung energy of the crystal that favors higher symmetry structures. Let us note that an addition of 4*d*- or 5*d*-metal dopants to V also affects the band-structure energy, due to the fact that they provide stronger hybridization but, as one can see from Table I for the case of V alloyed by Zr, Nb, and Hf, this effect is not as important as the change in the Madelung energy, but becomes compatible with the latter for the case of V alloyed with W and Mo, and even plays the dominant factor for the bcc structure stabilization in the V-Ta alloys.

The Madelung energy plays an opposite role (destabilization of the bcc phase) when 4*d*-Nb or 5*d*-Ta metals are alloyed with 3*d* metals (Ti, V, and Cr). Because of the abovementioned inherent difference between 4*d* and 5*d* states compared to the 3*d* states, there is a significant negative charge transfer on the Nb (Ta) atoms (see Tables III and IV) when Nb (Ta) is alloyed with 3*d* metals (Ti, V, and Cr). The large and negative charge transfers means that less charge is supplied into the interstitial region thereby decreasing the electrostatic Madelung energy contribution that favors destabilization of the high symmetry structure (the bcc phase). An addition of 3*d*-metal dopants to Nb (Ta) also affects the band-structure energy, due to the fact that they provide stronger hybridization, also contributing to destabilization of the bcc phase. Nevertheless, in spite of some negative contribution (due to alloying with 3*d* metals) to both ΔE_1 and ΔE_M, the Nb- and Ta-based alloys remain stable in the bcc structure due to the enough large value of ΔE_{tot} in pure metals (especially in Ta).

We have explained that the Madelung energy of the dilute alloy is increasing (decreasing) with the positive (negative) charge transfer on the host atoms and promoting (demoting) the stability of the bcc phase. Primarily this happens when orbitals with different quantum number belong to the constituents of the alloy. There is, however, another effect that may be playing a lesser role. In Table V we show the measured (room temperature[29]) and calculated equilibrium Wigner-Seitz radii of the studied elements. It is evident that the 3*d*-vanadium metal has the smaller atomic volume (or radius) than the 4*d* and 5*d* elements. This difference can influence the charge transfer between the constituents of the alloy or, using the terminology of Ref. 22, the "net charge" that originates from the redistribution of the electron density in the interstitial region between the atomic spheres.

Niobium and tungsten are the only metals under consideration that stabilize the bcc structure of Ta. Both Ta-Nb and

TABLE V. Calculated equilibrium Wigner-Seitz radius of bcc metals. Experimental data at room temperatures are shown in parentheses (Ref. 29). Notice that experimental data for the group-IVB metals (Ti, Zr, and Hf) correspond to the hcp structure.

Ti	V	Cr
3.035 (3.052)	2.799 (2.818)	2.655 (2.684)
Zr	Nb	Mo
3.334 (3.347)	3.089 (3.071)	2.949 (2.922)
Hf	Ta	W
3.298 (3.301)	3.115 (3.069)	2.976 (2.945)

Ta-W alloys have unlimited range of the bcc solid solutions.[30,31] It is well known that impurities and alloying can have a profound influence on the yield strength properties of a material.[32] Schwartz *et al.*[33] showed that adding 10 wt % (9.86 at. %) of W to Ta increases the yield strength of the materials, i.e., the minimum stress that is required to induce the plastic deformation, by more than a factor of 2. This observation was confirmed by Yang *et al.*[32] who calculated the elastic constants of the $Ta_{100-x}W_x$ alloys and successfully reproduced the experimental concentration behavior of the trigonal shear elastic constant, c_{44}.[34] Our calculations also confirm a gradual increase in the trigonal shear elastic constant, c_{44}, of the $Ta_{100-x}W_x$ alloys together with W content observed in Ref. 34. We also found a similar behavior in the $Ta_{100-x}Nb_x$ alloys as the amount of Nb in the alloy increases but this result requires experimental confirmation. Based on our results, we recommend alloying Ta with Nb for strengthening.

Finalizing the discussion section one should remember that the present calculations neither account for temperature effect nor the elastic energy contributions. As it was pointed out in Ref. 10, the softening of the shear elastic constants disappears as temperature increases. Account of the structural distortions could also influence the results presented in Table I. However, incorporation of both these effects in calculations is beyond capability of the ground state ($T=0$ K) formalism and thus out of the scope.

VI. CONCLUSIONS

To summarize, we have identified that the band-structure structure peculiarities are responsible for the Kohn anomaly on the transverse-acoustic-phonon mode TA [ξ00] of the group-VB transition metals and softening in their shear elastic constant with pressure. As far as reliable data on the phonon dispersions for V became recently available,[4] it is now become possible to verify predictions made in Refs. 9 and 10 that the nesting vector spanning two flat pieces of the FS of vanadium already exists at ambient pressure and leads to the Kohn anomaly on the transverse-acoustic-phonon mode TA [ξ00]. In the present study we prove that the length of the above-mentioned nesting vector matches the position where the Kohn anomaly (the maximum deviation from the elastic constant line) on the experimental TA [ξ00] phonon branch occurs. Our calculations confirm that this anomaly takes place at $\xi \approx 0.24$, 0.16, and 0.28 for V, Nb, and Ta, respectively, that is in a good accord with experimental observations.

For V this softening is associated with a phase transition to a rhombohedral phase close to 60 GPa while for Nb and Ta the bcc phase still remains stable at all studied pressures. The effect of alloying on the phase stability has been studied and three dominant mechanisms are recognized. First, the band-structure energy tends to destabilize or stabilize the bcc phase when a member of the group-VB is alloyed with its nearest neighbor from the same *d*-transition series to left or to the right, respectively. Second, the increase in both the electrostatic Madelung and band-structure energies remove softening and secure the bcc phase when vanadium metal is alloyed with neighboring elements from a higher *d*-transition series. Third, the decrease in both the electrostatic Madelung and band-structure energies causes some destabilization of the bcc phase when niobium or tantalum metals are alloyed with neighboring elements from the 3*d*-transition series although this destabilization is too small to cause a phase transition. Finally, a slight destabilization of the bcc phase occurs when niobium metal is alloyed with Hf or W or when tantalum metal is alloyed with Zr and Mo but both Nb and Ta remain stable in the bcc structure. The stability of the bcc phase is only strengthened when the "mixed" (4*d* and 5*d*) alloy has components from the same group-VB (the Nb-Ta system).

ACKNOWLEDGMENTS

Work performed under the auspices of the U.S. DOE by LLNL under Contract No. DE-AC52-07NA27344. Support from the Swedish Research Council (VR) is gratefully acknowledged by A.V.R., O.E.P., and L.V. A.L. would like to acknowledge A. Bosak for providing numerical data on the TA [ξ00] phonon branch for vanadium metal.

[1] M. Ishizuka, M. Iketani, and S. Endo, Phys. Rev. B **61**, R3823 (2000).

[2] N. Suzuki and M. Otani, J. Phys.: Condens. Matter **14**, 10869 (2002); J. Phys.: Condens. Matter **19**, 125206 (2007).

[3] W. Luo, R. Ahuja, Y. Ding, and H. K. Mao, Proc. Natl. Acad. Sci. U.S.A. **104**, 16428 (2007).

[4] A. Bosak, M. Hoesch, D. Antonangeli, D. L. Farber, I. Fischer, and M. Krisch, Phys. Rev. B **78**, 020301(R) (2008).

[5] Y. Ding, R. Ahuja, J. Shu, P. Chow, W. Luo, and H. K. Mao, Phys. Rev. Lett. **98**, 085502 (2007).

[6] A. K. Verma and P. Modak, EPL **81**, 37003 (2008).
[7] B. Lee, R. E. Rudd, J. E. Klepeis, P. Söderlind, and A. Landa, Phys. Rev. B **75**, 180101(R) (2007).
[8] S. L. Qiu and P. M. Marcus, J. Phys.: Condens. Matter **20**, 275218 (2008).
[9] A. Landa, J. Klepeis, P. Söderlind, I. Naumov, O. Velikokhatnyi, L. Vitos, and A. Ruban, J. Phys.: Condens. Matter **18**, 5079 (2006).
[10] A. Landa, J. Klepeis, P. Söderlind, I. Naumov, O. Velikokhatnyi, L. Vitos, and A. Ruban, J. Phys. Chem. Solids **67**, 2056 (2006).
[11] L. Koči, Y. Ma, A. R. Oganov, P. Souvatzis, and R. Ahuja, Phys. Rev. B **77**, 214101 (2008).
[12] A. Wexler and W. S. Corak, Phys. Rev. **85**, 85 (1952).
[13] V. V. Struzhkin, Y. A. Timofeev, R. J. Hemley, and H. K. Mao, Phys. Rev. Lett. **79**, 4262 (1997).
[14] B. T. Matthias, T. H. Geballe, and V. B. Compton, Rev. Mod. Phys. **35**, 1 (1963).
[15] Y. Nakagawa and A. D. B. Woods, Phys. Rev. Lett. **11**, 271 (1963).
[16] A. D. B. Woods, Phys. Rev. **136**, A781 (1964).
[17] A. Landa, P. Söderlind, A. V. Ruban, O. E. Peil, and L. Vitos, Phys. Rev. Lett. **103**, 235501 (2009).
[18] L. Vitos, *Computational Quantum Mechanics for Materials Engineers: The EMTO Method and Applications* (Springer-Verlag, London, 2007).
[19] J. P. Perdew, K. Burke, and M. Ernzerhof, Phys. Rev. Lett. **77**, 3865 (1996).
[20] J. S. Faulkner, Prog. Mater. Sci. **27**, 1 (1982).
[21] D. J. Chadi and M. L. Cohen, Phys. Rev. B **8**, 5747 (1973); S. Froyen, *ibid.* **39**, 3168 (1989).
[22] A. V. Ruban and H. L. Skriver, Phys. Rev. B **66**, 024201 (2002); A. V. Ruban, S. I. Simak, P. A. Korzhavyi, and H. L. Skriver, *ibid.* **66**, 024202 (2002).
[23] I. A. Abrikosov, S. I. Simak, B. Johansson, A. V. Ruban, and H. L. Skriver, Phys. Rev. B **56**, 9319 (1997).
[24] F. D. Murnaghan, Proc. Natl. Acad. Sci. U.S.A. **30**, 244 (1944).
[25] M. Mehl, B. M. Klein, and D. A. Papaconstantopoulos, in *Intermetallic Compounds: Principles and Practice*, edited by J. H. Westbrook and R. L. Fleisher (Wiley, London, 1995), Vol. 1, p. 195.
[26] J. Rath and A. J. Freeman, Phys. Rev. B **11**, 2109 (1975).
[27] A. Bosak (private communication).
[28] B. M. Powell, R. Martel, and A. D. B. Woods, Phys. Rev. **171**, 727 (1968); Can. J. Phys. **55**, 1601 (1977).
[29] H. L. Skriver, *The LMTO Method* (Springer-Verlag, Berlin, 1984), p. 262.
[30] R. Krishnan, S. P. Garg, and N. Krishamurthy, in *Binary Alloy Phase Diagrams*, 2nd ed., edited by T. B. Massalski (ASM International, Materials Park, OH, 1990), Vol. 3, p. 2772.
[31] R. Krishnan, S. P. Garg, and N. Krishamurthy, in *Binary Alloy Phase Diagrams*, 2nd ed., edited by T. B. Massalski (ASM International, Materials Park, OH, 1990), Vol. 3, p. 3438.
[32] L. Yang, H. Cynn, J.-H. Klepeis, J. Pask, and R. Rudd, Abstracts of APS Meeting, Portland, OR, March 2010 Bull. Am. Phys. Soc. **55**(2), 389 (2010).
[33] A. J. Schwartz, D. H. Lassila, and M. M. LeBlanc, Mater. Sci. Eng., A **244**, 178 (1998).
[34] C. E. Anderson and F. R. Brotzen, J. Appl. Phys. **53**, 292 (1982).